

## SYNTHESIS AND ELECTROCHEMICAL CHARACTERIZATION OF NEW $\text{Li}_2\text{O-P}_2\text{O}_5$ COMPOUNDS FOR SOLID ELECTROLYTES

Heri Jodi<sup>1,2,\*</sup>, Anne Zulfia Syahrial<sup>1</sup>, Sudaryanto<sup>2</sup>, EvvyKartini<sup>2</sup>

<sup>1</sup>*Department of Metallurgy and Materials Engineering, Faculty of Engineering, Universitas Indonesia, Kampus UI Depok, Depok 16424, Indonesia*

<sup>2</sup>*Center for Science and Technology of Advanced Materials, BATAN, KawasanPuspiptekSerpong, Setu, Tangerang Selatan, Banten 15314, Indonesia*

(Received: December 2016 / Revised: May 2017 / Accepted: November 2017)

### ABSTRACT

The solid electrolyte is of great interest owing to its potential to be applied in a wide variety of electrochemical devices. One of the most stable solid electrolytes is lithium phosphate ( $\text{Li}_3\text{PO}_4$ ). However, this compound has low enough conductivity to be applied to a device such as an electrolyte. A previous study has reported that the mixture of  $x\text{Li}_2\text{O-P}_2\text{O}_5$ , where  $x=2$ , has a greater conductivity than  $\text{Li}_3\text{PO}_4$ , while, when  $x=1$ , this yields an amorphous structure. In this study, new compositions of the  $x\text{Li}_2\text{O-P}_2\text{O}_5$  compounds, where  $1 \leq x \leq 2$ , were prepared through solid-state reactions. The prepared compounds were characterized using X-ray Diffraction Spectrometry (XRD), Scanning Electron Microscopy (SEM), and Electrochemical Impedance Spectroscopy (EIS) measurements in order to investigate their structure, morphology, and electrochemical properties. The XRD characterization showed that both of the samples were composed mainly of  $\text{Li}_4\text{P}_2\text{O}_7$  crystals. Agglomeration of particles was observed in the samples. The conductivity of the compounds was of the order of  $10^{-6}$  S/cm, which was higher by three orders of magnitude than that of  $\text{Li}_3\text{PO}_4$ . The evaluated power exponent of conductivity indicated that the long-range drift of ions may be one of the sources of ion conduction in both of the observed samples. The nature of the dielectric loss indicated that the conduction in the samples was more predominantly DC conduction.

*Keywords:* Solid electrolytes;  $\text{Li}_2\text{O-P}_2\text{O}_5$ ; Electrochemical impedance spectrometry; Conductivity; Dielectric

### 1. INTRODUCTION

The electrolyte is one of the main components in a battery, and serves as an ion-conducting medium within the cell. Conventional electrolytes consist of dissolved lithium salt in an organic solvent. The usage of this type of liquid electrolyte is believed to be one cause of the irreversible loss of capacity that cannot be regained, due to the formation of an unstable layer in the electrode-electrolyte interfaces (Agubra & Fergus, 2014). Such electrolytes also limit the battery lifecycle, restrict the service temperature, and prompt leakages and security issues (Kotobuki, 2012). The replacement of conventional liquid electrolytes with a non-flammable solid form is of great interest and importance as it may enable these problems to be overcome.

There are several advantages to applying solid electrolytes in an electrochemical device; these include not causing leakages or pollution, and exhibiting better resistance to heat, shock, and

---

\*Corresponding author's email: heri.jodi@ui.ac.id, Tel: +62-21-786 3510, Fax: +62-21-787 2350  
Permalink/DOI: <https://doi.org/10.14716/ijtech.v8i8.681>

vibration than liquid electrolytes (Sahu et al., 2014). Moreover, the solid electrolyte is a single-ion-conductor that only transmits one species of carriers. Therefore, during its service, there is almost no concentration gradient in the cell, which is very useful in diminishing the potency of cell overpotential (Quartarone&Mustarelli, 2011).

Phosphate oxide-based solid electrolytes are widely investigated because of their favorable properties; for example, they exhibit a strong glass-forming character, low melting point, and simple composition. Lithium phosphate ( $\text{Li}_3\text{PO}_4$ ) is one of the most stable phosphate oxide-based solid electrolytes. However, this compound has a sufficiently low conductivity to be applied to a cell, due to the high bulk resistance. Hence,  $\text{Li}_3\text{PO}_4$  is widely used in the form of a thin layer in order to reduce the resistance value (Senevirathne et al., 2013). This material can be prepared either through the conventional solid-state reaction or a wet chemical reaction (Jodi et al., 2016). Some investigations of solid electrolytes have been reported; these have utilized methods such as morphological characterization, structural investigation using X-ray Diffraction Spectrometry (XRD) characterization (Nur et al., 2016), the neutron diffraction method (Jahja et al., 2015), and a computer simulation involving the first-principles modeling technique (Lepley&Holzwarth, 2012). Many studies that aim to improve the conductivity of phosphate oxide-based electrolytes have been reported. Some of these approaches included mixing different kinds of anions (Yi et al., 2014), providing halide metal dopant (Zaafouri et al., 2014), and preparing a composite (Jodi et al., 2016).

Some studies on the conductivity of  $x\text{Li}_2\text{O}-\text{P}_2\text{O}_5$  compounds at the stoichiometric composition of  $x = 1\sim 5$  have been reported (Kartini et al., 2014; Jahja et al., 2015; Jodi et al., 2016). When  $x=1$ , the compound was reported to form an amorphous phase, while for  $x=2$  and  $x=3$  the compound formed crystalline phases. For  $\text{Li}_2\text{O}$  content, at less than  $x\approx 1.3$ , the compound was reported to construct  $\text{LiPO}_3$  phases which could be quenched to a glass form (Nakano et al., 1979). The highest reported conductivity was reached by the compound where  $x=2$ . Although the studies reported various compositions, there were no findings provided regarding the conductivity of a non-stoichiometric composition of amorphous and crystalline phases.

In this work, new non-stoichiometric compositions of  $x\text{Li}_2\text{O}-\text{P}_2\text{O}_5$  were prepared through a solid-state reaction, to be used as a solid electrolyte. The study was focused on electrochemical characterization in order to determine the electrochemical properties of the  $x\text{Li}_2\text{O}-\text{P}_2\text{O}_5$  compounds where  $x=1.5$  and  $x=1.8$ . Synthesized samples were characterized using XRD, Scanning Electron Microscopy (SEM), and Electrochemical Impedance Spectroscopy (EIS) characterization. The XRD patterns confirmed characteristic peaks of  $\text{Li}_4\text{P}_2\text{O}_7$  in both samples. The conductivity of the compounds was of the order of  $10^{-6}$  S/cm. Although the compounds contained less  $\text{Li}_2\text{O}$  content, their conductivity was of the same order as that of stoichiometric  $\text{Li}_4\text{P}_2\text{O}_7$ , and was higher by three orders of magnitude than that of  $\text{Li}_3\text{PO}_4$ .

## 2. EXPERIMENTAL

Lithium carbonate ( $\text{Li}_2\text{CO}_3$ , Alfa Caesar, 99%) and ammonium dihydrogen phosphate ( $\text{NH}_4\text{H}_2\text{PO}_4$ , Merck, 98%) were used as initial materials to prepare the  $x\text{Li}_2\text{O}-\text{P}_2\text{O}_5$  compounds for  $x=1.5$  and  $x=1.8$ , using the conventional melt-quenching method. Ceramic crucibles, a digital scale, an agate mortar, magnetic stirrers, and a heating furnace were employed in preparing the samples.

The non-stoichiometric molar ratios of  $\text{Li}_2\text{CO}_3$  and  $\text{NH}_4\text{H}_2\text{PO}_4$  were well mixed using magnetic stirrers for two hours, and were ground for an hour. The homogenized powder batches were calcined at 673 K for an hour in order to release  $\text{H}_2\text{O}$ ,  $\text{NH}_3$ , and  $\text{CO}_2$ , and then were gradually heated up to 923 K for four hours. The mixtures were then quenched in demineralized water and smoothed in an agate mortar.

A Shimadzu XD-610 XRD, equipped with a  $\text{Cu K}\alpha_1$  source target, was utilized to record the room-temperature XRD pattern of the samples and confirmed material formation. Diffraction patterns were logged with a goniometer ( $2\theta$ ) from  $5^\circ$  to  $90^\circ$ . A JEOL JSM-6510LA SEM, equipped with Energy Dispersive X-ray Spectrometry (EDS), was employed to observe the morphology and provide an elemental analysis of the samples.

To characterize the electrochemical properties, the resulting products were pelletized into 15 mm diameter cylindrical forms using 15 MPa uniaxial pressures, and were heated from room temperature to 923 K for four hours. Silver paste was applied on both sides of the samples to serve as ion-blocking electrodes and current collectors. Impedance spectra were collected in an ambient atmosphere and temperature at an applied voltage of 1 V over a frequency range of 42 Hz–5 MHz using a HIOKI LCR HiTESTER 3532-50.

### 3. RESULTS AND DISCUSSION

XRD spectra of the  $x\text{Li}_2\text{O}-\text{P}_2\text{O}_5$  compounds where  $x=1.5$  and  $x=1.8$  are shown in Figure 1. The crystal phases of both of the compounds are mainly identified as  $\text{Li}_4\text{P}_2\text{O}_7$  phases indexed by anorthic symmetry with P-1 space group (#98-005-9243). The characteristic peaks of this phase present at  $2\theta = 20.5^\circ$ ,  $22.5^\circ$ , and  $27.8^\circ$ , which corresponds to (0-11), (01-2), and (020) reflections respectively in both spectra. The characteristic reflections of the  $\text{Li}_4\text{P}_2\text{O}_7$  phase are more present in the spectra of the compound where  $x=1.8$ , as shown in Figure 1b. The highest peak, at  $2\theta = 20.5^\circ$ , has a full width at half maximum value of 0.128 and a crystallite size of 969.3 Å. In addition, two minor phases were found and identified as  $\gamma\text{-Li}_3\text{PO}_4$  and  $\text{LiPO}_3$  phases. The compound where  $x=1.8$  has fewer minor phases than the compound where  $x=1.5$ .

Although the two  $\text{Li}_2\text{O}-\text{P}_2\text{O}_5$  compounds differ in terms of their stoichiometry and Li content, they exhibit the same lattice structure and nearly the same crystallization kinetics. These findings are in agreement with earlier research which reported that, at a temperature above 873 K,  $x\text{Li}_2\text{O}-\text{P}_2\text{O}_5$  compounds will form  $\text{Li}_4\text{P}_2\text{O}_7$  phases in the range of  $1.3 \leq x \leq 2$ , and only differ in melting temperature, which increases with lithium content (Nakano et al., 1979). Furthermore, due to a rapid and reversible polymorphic inversion at about 900 K, the high-temperature  $\text{Li}_4\text{P}_2\text{O}_7$  form could not be obtained by quenching (Tien & Hummel, 1961). Therefore, the presence of minor phases in the spectra is predicted to be an effect of the quenching methods used in this experiment. A longer heating time to complete the reaction and natural cooling are expected to potentially diminish the presence of the minor phases.

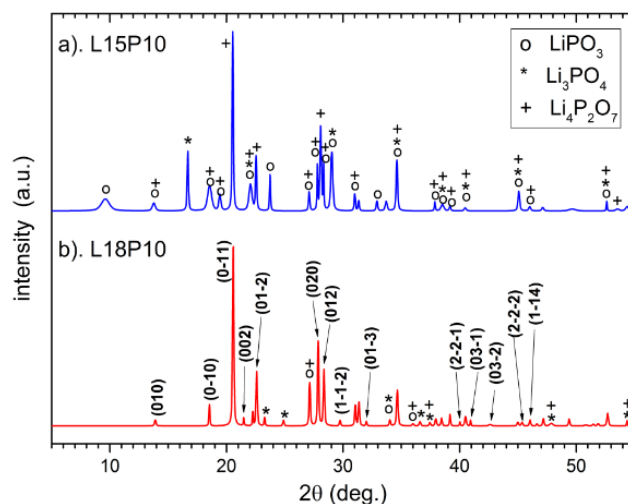


Figure 1 XRD pattern of  $x\text{Li}_2\text{O}-\text{P}_2\text{O}_5$  compounds: (a)  $x=1.5$ ; and (b)  $x=1.8$

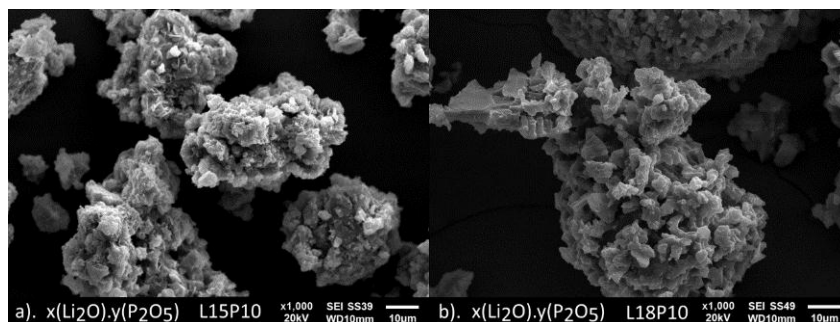


Figure 2 The SEM micrographs of  $x\text{Li}_2\text{O}-\text{P}_2\text{O}_5$  compounds:(a)  $x=1.5$ ; and (b)  $x=1.8$

Figure 2 shows the SEM micrographs of the  $x\text{Li}_2\text{O}-\text{P}_2\text{O}_5$  compounds where  $x=1.5$  and  $x=1.8$ . It is clearly shown that both compounds have nearly the same structure, consisting of porous agglomerates. The formation of these agglomerates indicates that the compounds have particles that are smaller than the size shown in micrographs. These agglomerates are thought to form during the gradual heating process (Jodi et al., 2016). Agglomerates of the compound where  $x=1.8$  appear to be more solid with a size of about 48-110  $\mu\text{m}$ , much larger than that of the compound where  $x=1.5$ , which is about 8-60  $\mu\text{m}$ . This difference is believed to be due to the difference in melting temperature of the precursors of the compounds:  $\text{P}_2\text{O}_5$  has a lower melting temperature than  $\text{Li}_2\text{O}$ . The addition of  $\text{Li}_2\text{O}$  content leads to more  $\text{Li}_2\text{O}$  particles in the melted  $\text{P}_2\text{O}_5$ , resulting in enlargement of the size of the agglomerates.

Quantitative analysis using EDS provided the elemental composition of the samples, which were dominated by the elements O and P, confirming the formation of the  $\text{Li}_2\text{O}-\text{P}_2\text{O}_5$  polymorphs. The ratio of the atomic composition of O and P was in the range 3.1–3.5, which means that both samples were dominated by  $\text{Li}_4\text{P}_2\text{O}_7$  as indicated by the XRD results.

The impedance plots for the  $x\text{Li}_2\text{O}-\text{P}_2\text{O}_5$  compounds where  $x=1.5$  and  $x=1.8$  at room temperature are presented in Figure 3a. The impedance plots for the two compounds have the same nature; each consists of a depressed semicircle, which is indicative of a non-Debye relaxation process. The presence of a single semicircle indicates that the electrical processes in the material essentially arise due to the contribution of the bulk material (Taher et al., 2016). The bulk resistance,  $R_b$ , of the electrolytes is determined according to the interception of an extrapolated semicircle with a real axis (Chilaka& Ghosh, 2014). The value of  $R_b$  is observed to increase with the addition of  $\text{Li}_2\text{O}$ , as presented in Table 1.

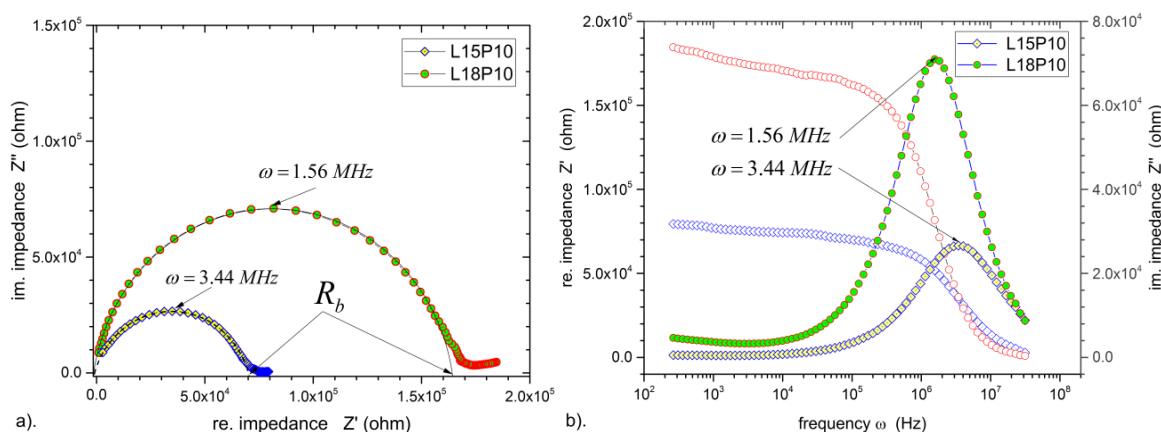


Figure 3 Room temperature complex impedance and frequency dependence (Bode) of complex impedance plots of  $x\text{Li}_2\text{O}-\text{P}_2\text{O}_5$  compounds. Blank marks in the Bode plots are for resistive( $Z'$ ), while filled marks are for capacitive impedance ( $Z''$ )

Table 1 The bulk resistance and fitted conductivity parameters for the  $x\text{Li}_2\text{O-P}_2\text{O}_5$  compounds calculated from the observed experimental impedance values

$x\text{Li}_2\text{O-P}_2\text{O}_5$	Resistance $R_b(\text{ohm})$	DC conductivity $\sigma_{dc}(\text{S/cm})$	Power law exponent(s)
x=1.5	$7.01 \times 10^{+4}$	$4.09 \times 10^{-6}$	0.76
x=1.8	$1.64 \times 10^{+5}$	$1.11 \times 10^{-6}$	0.69

The presentation of the complex impedance data as a function of angular frequency is shown in Figure 3b. The variation of resistive impedance ( $Z'$ ) with frequency demonstrates that the value of  $Z'$  increases with the addition of  $\text{Li}_2\text{O}$  content. At high frequency, the  $Z'$  values of both samples coincide, implying the possible release of space charge as a result of a reduction in the resistive behavior of the material. The variation of capacitive impedance ( $Z''$ ) with frequency shows that the value of  $Z''$  for both of the samples attains a maximum ( $Z''_{\text{max}}$ ) at a certain frequency, which explains the presence of a relaxation process in the sample (Subohi et al., 2016). In dielectric material, a relaxation process generally occurs due to the presence of immobile charges at low temperature (Jonscher, 1977). The maximum value of  $Z''$  increases with an increase in  $\text{Li}_2\text{O}$  content, indicating an increase in resistance and a decrease in capacitance. The relaxation time, which is the inverse of the frequency at which  $Z''$  attains a maximum, increases with the rise in the value of  $x$ .

The complex conductivity of the samples varies with angular frequency (Jonscher, 1977), and could be calculated from the measured impedance value and dimensions of the samples. The variation of complex conductivity as a function of frequency for the  $x\text{Li}_2\text{O-P}_2\text{O}_5$  compounds where  $x=1.5$  and  $x=1.8$  are shown in Figure 4. It can be observed that the conductivity pattern could be divided into two regions, that is, an almost frequency-independent region for low-frequency, and the high-frequency region in which conductivity increases in parallel with the increase in frequency. The most level region of conductivity in the lower frequency characterizes the direct conductivity that is a result of the displacement of charge carriers (Jayswal et al., 2013). In the higher frequency region, the conductivity obeys Jonscher's power law,  $A\omega$ , which indicates the presence of a hopping conduction mechanism (Sassi et al., 2015).

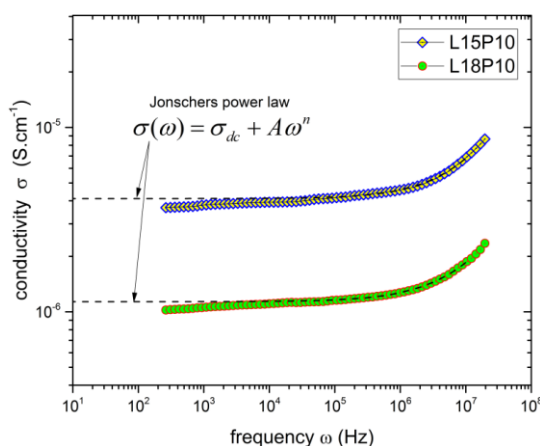


Figure 4 The room-temperature frequency-dependent plots of complex conductivity for  $x\text{Li}_2\text{O-P}_2\text{O}_5$  compounds with  $x=1.5$  and  $x=1.8$

The observed complex conductivity curves can be described by Jonscher's power law equation, as follows (Jonscher, 1977):

$$\sigma(\omega) = \sigma_{dc} + A\omega^s \tag{1}$$

where  $\sigma_{dc}$ ,  $A$ , and  $s$  are the DC conductivity, the temperature-dependent factor, and the power law exponent, respectively. The conductivity parameters can be obtained by fitting the curve to Equation 1 using the non-linear least squares fitting procedure, as presented in Table 1. It is evident that DC conductivity decreases with the addition of  $\text{Li}_2\text{O}$  from  $x=1.5$  to  $x=1.8$ . However, both of the compounds have DC conductivity in the same order, that is, of  $10^{-6}$  S/cm. This value of conductivity is of the same order as the conductivity of stoichiometric  $\text{Li}_4\text{P}_2\text{O}_7$ , which contains more  $\text{Li}_2\text{O}$  content, but three orders higher than the conductivity of  $\text{Li}_3\text{PO}_4$  where  $x=3$  (Jodi et al., 2016). The increase in conductivity may be ascribed either to the increase in mobile ion concentration or to the increase in free space, which allows the ions to move. The values of the evaluated power law exponent ( $s$ ) are in the range of 0.69–0.76 for both compounds, indicating that, for each of the compounds, the backward hopping is slower than the site relaxation time. Consequently, the hopping of lithium ions may be one of the sources of conduction in this  $x\text{Li}_2\text{O}-\text{P}_2\text{O}_5$  system of  $\text{Li}_4\text{P}_2\text{O}_7$  (Taher et al., 2016).

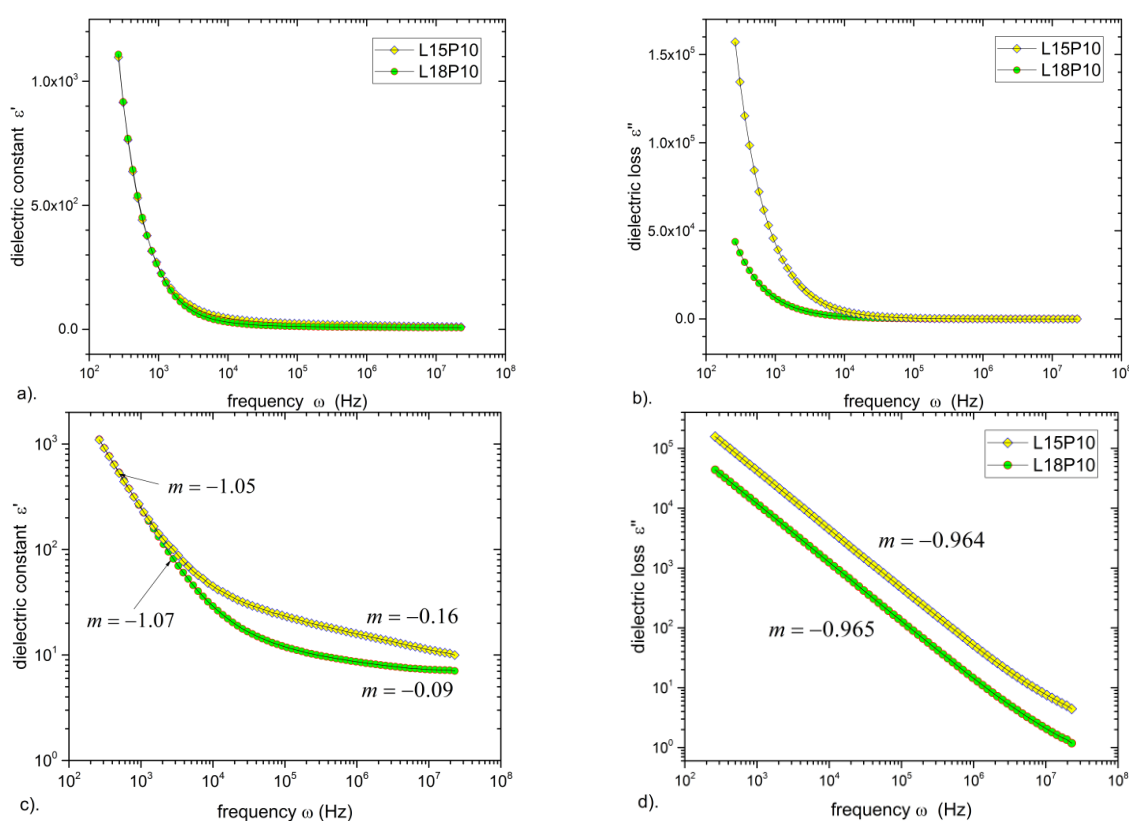


Figure 5 Frequency-dependent plots of permittivity for  $x\text{Li}_2\text{O}-\text{P}_2\text{O}_5$  compounds

Figure 5 shows the frequency-dependent plots for the permittivity of the  $x\text{Li}_2\text{O}-\text{P}_2\text{O}_5$  compounds, where 5a and 5b show the normal view, and 5c and 5d show the log-log view. The real part of complex permittivity is the dielectric constant ( $\epsilon'$ ), while the imaginary part is the dielectric loss ( $\epsilon''$ ). In both parts of permittivity, a very strong dispersion is observed in the low-frequency range. With regards to the dielectric material, this effect is due to the significant contribution of charge polarization at the electrode–electrolytes interfaces for the dielectric constant, while, for the dielectric loss, the dispersion is due to the migration of ions in the material (Adnan & Mohamed, 2012). At higher frequency, an almost frequency-independent nature is observed in both the dielectric constant and dielectric loss. This is due to the rapid periodic electric field reversal and

to the limitation of ion vibrations, respectively. The log-log plot permittivity provides clear evidence that the value of both parts of the permittivity of the compounds where  $x=1.5$  are higher than those of  $x=1.8$ . According to the theory of hopping of charge carriers over a potential barrier between charged defects, the slope of dielectric loss is inversely proportional to the maximum barrier height (Mott & Davis, 2012). Thus, both of the compounds have the same barrier height, although they have different compositions. The values of the slope ( $m$ ) are near minus unity, which indicates that the conduction in both samples was more predominantly DC conduction.

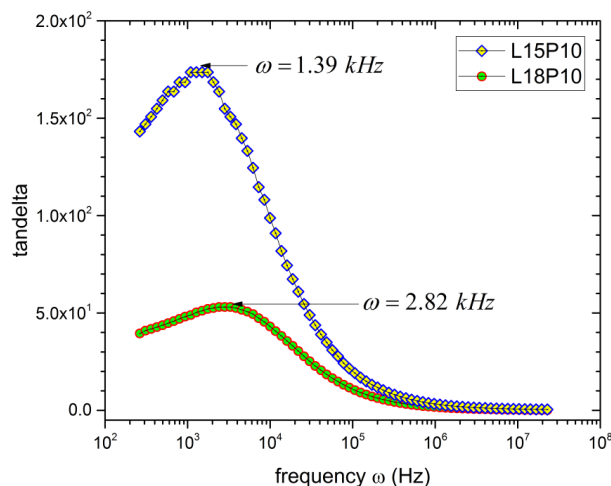


Figure 6 Frequency-dependent plots of tandelta for  $x\text{Li}_2\text{O}-\text{P}_2\text{O}_5$  compounds

Figure 6 presents the frequency-dependent plots of tandelta for the  $x\text{Li}_2\text{O}-\text{P}_2\text{O}_5$  compounds where  $x=1.5$  and  $x=1.8$ . The peak of tandelta is shifted toward a higher frequency, as the content of  $\text{Li}_2\text{O}$  increases from  $x=1.5$  to  $x=1.8$ . The peak of tandelta is expected to occur when the hopping frequency is approximately equal to the applied external field, and the frequency of the electric field is expected to be proportional to the jumping probability per unit time (Hockicko et al., 2015). Thus, the shift of the peak toward a higher frequency indicates that the jumping probability increases with the addition of  $\text{Li}_2\text{O}$  content, and also with the content of mobile ions in the compounds (Sudaryanto et al., 2015).

#### 4. CONCLUSION

In this current work, we have successfully synthesized  $x\text{Li}_2\text{O}-\text{P}_2\text{O}_5$  compounds where  $x=1.5$  and  $x=1.8$  by using a solid-state reaction. The XRD spectral data indicated that all of the compounds were composed mainly of  $\text{Li}_4\text{P}_2\text{O}_7$  crystals. Minor phases of  $\text{LiPO}_3$  and  $\text{Li}_3\text{PO}_4$  were present in both compositions, but more phases were found in the composition where  $x=1.5$ . The two compounds had the same agglomerated structure, but the compound where  $x=1.5$  had a smaller agglomerate size. The impedance spectra of the two compounds had the same characteristics, although the compound where  $x=1.5$  had lower resistance, and hence better conductivity. The DC conductivity of both compounds was of the order of  $10^{-6}$  S/cm, which was higher by three orders of magnitude than that of  $\text{Li}_3\text{PO}_4$ . The value of the AC-conductivity parameters for the higher frequency revealed that the long-range drift of ions may be one of the sources of ion conduction in the compounds.

#### 5. ACKNOWLEDGEMENT

Financial support from the Ministry of Research, Technology, and Higher Education of the Republic of Indonesia through the Research Grant No. 278/SP2H/LT/DRPM/III/2016 is gratefully acknowledged. The authors would like to thank the Center for Science and Technology

of Advanced Materials, the National Nuclear Energy Agency and the Department of Metallurgy and Materials Engineering, Universitas Indonesia for the great support.

## 6. REFERENCES

- Adnan, S.B.R.S., Mohamed, N.S., 2012. Conductivity and Dielectric Studies of  $\text{Li}_2\text{ZnSiO}_4$  Ceramic Electrolyte Synthesized via Citrate Sol-Gel Method. *International Journal of Electrochemical Science*, Volume 7(10), pp. 9844-9858
- Agubra, V.A., Fergus, J.W., 2014. The Formation and Stability of the Solid Electrolyte Interface on the Graphite Anode. *Journal of Power Sources*, Volume 268, pp. 153-162
- Chilaka, N., Ghosh, S., 2014. Dielectric Studies of Poly (Ethylene glycol)-Polyurethane/Poly (Methylmethacrylate)/Montmorillonite Composite. *Electrochimica Acta*, Volume 134, pp. 232-241
- Hockicko, P., Kudelcik, J., Munoz, F., Munoz-Senovilla, L., 2015. Structural and Electrical Properties of  $\text{LiPO}_3$  Glasses. *Advances in Electrical and Electronic Engineering*, Volume 13(2), pp. 198-205
- Jahja, A.K., Putra, T.Y.S.P., Mugirahardjo, H., Supardi, Insani, A., Kartini, E., 2015. Structural Analysis of Electrolytic Material  $(\text{Li}_2\text{O})_x(\text{P}_2\text{O}_5)_y$  ( $x=5, y=1$ ) with High Resolution Neutron Diffraction Method (*Analisis Struktural Bahan Elektrolit  $(\text{Li}_2\text{O})_x(\text{P}_2\text{O}_5)_y$  ( $x=5, y=1$ ) dengan Metode Difraksi Neutron Resolusi Tinggi*). In: Prosiding Seminar Nasional Hamburan Neutron dan Sinar-X 2015. pp. 23-31, Serpong, 6-7 October, Indonesia (in Bahasa)
- Jayswal, M.S., Kanchan, D.A., Sharma, P., Gondaliya, N., 2013. Relaxation Process in  $\text{PbI}_2\text{-Ag}_2\text{O-V}_2\text{O}_5\text{-B}_2\text{O}_3$  System: Dielectric, AC Conductivity, and Modulus Studies. *Materials Science and Engineering B*, Volume 178(11), pp. 775-784
- Jodi, H., Zulfia, A., Deswita, Kartini, E., 2016. A Study of the Structural and Electrochemical Properties of  $\text{Li}_3\text{PO}_4\text{-MMT-PVDF}$  Composites for Solid Electrolytes. *International Journal of Technology*, Volume 7(8), pp. 1291-1300
- Jodi, H., Supardi, Kartini, E., Zulfia, A., 2016. Synthesis and Electrochemical Characterization of  $\text{Li}_3\text{PO}_4$  for Solid State Electrolytes. *Jurnal Sains Materi Indonesia*, Volume 18(1), pp.1-8
- Jonscher, A.K., 1977. The 'Universal' Dielectric Response. *Nature*, Volume 267(5613), pp.673-679
- Kartini, E., Honggowiranto, W., Supardi, Jodi, H., Jahja, A.K., Wahyudianingsih, 2014. Synthesis and Characterization of New Solid Electrolyte Layer  $(\text{Li}_2\text{O})_x(\text{P}_2\text{O}_5)_y$ . In: Proceedings of the 14<sup>th</sup> Asian Conference on Solid State Ionics 2014. pp. 163-173
- Kotobuki, M., 2012. The Current Situation and Problems of Rechargeable Lithium-ion Batteries. *The Open Electrochemistry Journal*, Volume 4, pp. 28-35
- Lepley, N.D., Holzwarth, N.A.W., 2012. Computer Modeling of Crystalline Electrolytes: Lithium Thiophosphates and Phosphates. *Journal of The Electrochemical Society*, Volume 159(5), pp. A538-A547
- Mott, N.F., Davis, E.A., 2012. *Electronic Processes in Non-Crystalline Materials 2<sup>nd</sup>*. New York: Oxford University Press
- Nakano, J., Yamada, T., Miyazawa, S., 1979, Phase Diagram for a Portion of the System  $\text{Li}_2\text{O-Nd}_2\text{O}_3\text{-P}_2\text{O}_5$ . *Journal of the American Ceramic Society*, Volume 62(9-10), pp. 465-467
- Nur I.P.A., Kartini, E., Prayogi, L.D., Faisal, M., Supardi, 2016. Crystal Structure Analysis of  $\text{Li}_3\text{PO}_4$  Powder Prepared by Wet Chemical Reaction and Solid State Reaction by using X-Ray Diffraction (XRD). *Ionics*, Volume 22(7), pp. 1051-1057
- Quartarone, E. Mustarelli, P., 2011. Electrolytes for Solid-state Lithium Rechargeable Batteries: Recent Advances and Perspectives. *Chemical Society Reviews*, Volume 40(5), pp. 2525-2540
- Sahu, G., Lin, Z., Li, J., Liu, Z., Dudney, N., Liang, C., 2014. Air-stable, High-conduction Solid Electrolytes of Arsenic-substituted  $\text{Li}_4\text{SnS}_4$ . *Energy & Environmental Science*, Volume 7(3),



pp. 1053–1058

- Sassi, M., Bettaibi, A., Oueslati, A., Khirouni, K., Gargouri, M., 2015. Electrical Conduction Mechanism and Transport Properties of  $\text{LiCrP}_2\text{O}_7$  Compound. *Journal of Alloys and Compounds*, Volume 649, pp. 642–648
- Senevirathne, K., Day, C.S., Gross, M.D., Lachgar, A., Holzwarth, N.A.W., 2013. A New Crystalline LiPON Electrolyte: Synthesis, Properties, and Electronic Structure. *Solid State Ionics*, Volume 233, pp. 95–101
- Subohi, O., Bowen, C.R., Malik, M.M., Kurchania, R., 2016. Dielectric Spectroscopy and Ferroelectric Properties of Magnesium Modified Bismuth Titanate Ceramics. *Journal of Alloys and Compounds*, Volume 688, pp. 27–36
- Sudaryanto, Yulianti, E. Jodi, H., 2015. Studies of Dielectric Properties and Conductivity of Chitosan-Lithium Triflate Electrolyte. *Polymer-Plastics Technology and Engineering*, Volume 54(3), pp. 290–295
- Taher, Y.B., Moutia, N., Oueslati, A., Gargouri, M., 2016. Electrical Properties, Conduction Mechanism, and Modulus of Diphosphate Compounds. *RSC Advances*, Volume 6(46), pp. 39750–39757
- Tien, T.Y., Hummel, F.A., 1961. Studies in Lithium Oxide Systems: X, Lithium Phosphate Compounds. *Journal of the American Ceramic Society*, Volume 44(5), pp. 206–208
- Yi, E., Wang, W., Mohanty, S., Kieffer, J., Tamaki, R., Laine, R.M., 2014. Materials that can Replace Liquid Electrolytes in Li Batteries: Superionic Conductivities in  $\text{Li}_{1.7}\text{Al}_{0.3}\text{Ti}_{1.7}\text{Si}_{0.4}\text{P}_{2.6}\text{O}_{12}$ , Processing Combustion Synthesized Nanopowders to Free Standing Thin Films. *Journal of Power Sources*, Volume 269, pp. 577–588
- Zaafouri, A., Megdiche, M. Gargouri, M., 2014. AC Conductivity and Dielectric Behavior in Lithium and Sodium Diphosphate  $\text{LiNa}_3\text{P}_2\text{O}_7$ . *Journal of Alloys and Compounds*, Volume 584, pp. 152–158